4-9-2007

Influence of Evapotranspiration on Patterns of Ground-Water Conductivity in Small Basins

Ana Jiménez
University of South Florida

Influence of Evapotranspiration on Patterns of Ground-Water Conductivity in Small Basins

by

Ana Jiménez

A thesis submitted in partial fulfillment
of the requirements for the degree of
Master of Science
Department of Geology
College of Arts and Science
University of South Florida

Major Professor: Mark T. Stewart, Ph.D.
Sarah Kruse, Ph.D.
Mark C. Rains, Ph.D.

Date of Approval:
April 9, 2007

Keywords: evapotranspiration, ground-water conductivity, MODFLOW, MT3D.

Dedication

Para Aitite.

… te debo una comida…

Acknowledgments

I would like to thank Dr. Stewart for being my advisor, teaching me and giving me all the help I needed to do this project. Thank you to Dr. Kruse and Dr. Rains for guiding me as committee members. Also thanks to Swagata Guha and Robert Degraaf for giving me a hand with the fieldwork and Mikel Diez for helping me anytime I asked. Finally thank you to Tampa Bay Water for let us work in their area and also for being so helpful providing information.

Table of Contents

List of Figures

List of Tables

Influence of Evapotranspiration on Patterns of

Ground-Water Conductivity in Small Basins

Ana Jiménez

ABSTRACT

Ground-water conductivity data were obtained from shallow wells in a 12 km^2 stream-basin along a 400 m transect, extending from the divide to the stream. The stream, Pringle Branch, is a second-order perennial stream in Hillsborough County, Florida. The shallow stratigraphy consists of 2-3 m of fine sand over a layer of clayey silt and silty clay. Vegetation cover includes grasses on the upper and middle slope, and riparian woodlands on the foot slope and floodplain. Precipitation is about 1.3 m per year. Shallow ground-water conductivity is about 50 uS/cm at the divide. It increases moderately along the mid slope, then increases markedly within the riparian woodlands, reaching a maximum of about 500 uS/cm at 30m from the stream and then decreases to about 150 uS/cm at the stream. The spatial variation of terrain electrical conductivity data collected using electromagnetic methods (EM 31) is similar to the spatial variation of ground-water conductivity. Dry season through wet season monitoring shows that ground-water conductivity in each well varies about 40 %, generally following variations in potential evapotranspiration (ET_{pan}). The more than five-fold increase in ground-water conductivity from divide to riparian woodlands is maintained during both dry and wet

seasons. The ground-water conductivity in this basin appears to be determined principally by spatial variations in ET and not by temporal variations in ET or interaction with soil minerals. The data suggest that patterns of ground-water conductivity can be used to infer patterns of ET variation within a small basin. A mass transport model constructed to test the hypothesis that evapotranspiration has the dominant effect on ground-water conductivity closely duplicates the observed variation in ground-water conductivity from divide to stream. The model uses two evaporation rates, 0.73 m/y for the grasses and 1.46 m/y for the riparian woodlands, and no contribution from solution of matrix materials.

1. Introduction

Estimation of evapotranspiration (ET) rates in small drainage basins is a critical element in calibration of numerical models used for water-resources management. To date, ET rates are directly measured by monitoring soil moisture or calculated from detailed vertical profiles of temperature, relative humidity and wind speed. ET rates are also estimated from more general measurements of climatic data, by land use and vegetative cover, or commonly, as a calibration variable in numerical models.

Direct measurements are expensive and are often impracticable to use for regional or even sub-regional studies. The estimation methods suffer from a lack of calibration to direct measurements. It would be useful to have a method for determination of ET that is more locally representative and accurate than the estimation methods, but less expensive and time consuming than the current direct-measurement methods.

The mass balance method has been used in many studies to estimate base-flow contribution to streams (O'Brien & Hendershot, 1993; Laudon & Slaymaker, 1997). In most studies, the contribution of evapotranspiration to the total dissolved solids (TDS) content of ground water has not been considered. ET removes water from soils and the water table, but leaves the solutes behind. As ET is about four-fifths of the hydrologic budget in west-central Florida (100 cm out of 130 cm) (Nachabe et al. 2005), ET should increase the solute concentration of the original recharge waters by a factor of five, in addition to any increase in solute concentration from soil-water interactions. This

suggests that measurements of the conductivity of shallow ground water may provide a method for determining relative ET rates and the spatial variation of ET. This ET value would be an integrated value for ET from the unsaturated zone and the water table.

This study uses a numerical model, calibrated to field data from a small drainage basin, to investigate the relative contributions of ET and soil/water interactions to the TDS content of shallow ground water in small basins.

1.1. Previous work

Many different approaches have been followed to estimate ET. One approach involves techniques based on the gain of water vapor by the atmosphere. One of these is the Penman-Monteith method used in studies such as Allen et al. (1989) and Kite (2000). This method is a combination of the Penman equation (Penman, 1948), which combines the energy required to sustain the evaporation and an empirical description of the diffusion mechanism, with a different resistance factor for each crop surface. ET can also be determined by eddy-correlation measurements based in the correlation between turbulent motions of the air and the specific humidity of the air (Swinbank, 1951; Lund & Soegaard, 2003). Bowen (1926) and Yoshimasa et al. (2000) calculated ET by the ratio of energy available for sensible heating to energy available for latent heating that is, the Bowen ratio. With the availability of large amounts of data and increased computing power, remote sensing data sets and multispectral satellite images are also used to calculate ET over large scales (Kite & Droogers, 1999; Roerink et al., 2000).

Another approach involves techniques based on the rate of loss of liquid water from the surface. ET rates are estimated based on diurnal ground water level fluctuations (Dolan et al., 1984; and Bauer et al., 2003), using lysimeters and evaporation pans (Mao et al., 2002) and quantifying the evaporation losses analyzing recession curves (Wittenberg & Sivapalan, 1999). As all these methods are expensive and require long calculations, this study proposes a more efficient way to estimate relative ET rates and spatial variations based on ground-water conductivity.

1.2. General approach.

This study investigates the possibility that the relationship between ground-water conductivity and ET could lead to the development of a new method to estimate ET based on ground-water conductivity. For that purpose, the study is focused on understanding better the relationship between these two variables. This problem is approached by gathering and measuring ground-water and ET data from a small basin in central Florida. These data are then analyzed and used to constrain an advection-dispersion model that describes the mass transport through this basin. This model is solved numerically to quantify the effect of ET on ground-water conductivity.

2. Conceptual model

The conceptual model of the system consists of a vertical profile of the basin (Fig. 1). The upslope end is a recharge divide and the stream is a discharge divide. The lower boundary of the model is a no-flow boundary defined by a layer of low permeability. According to previous studies (Stewart et al., 2006) lateral flows into the system can be assumed to be negligible as the profile is assumed to be along a flowline. The upper boundary of the system is defined by the land surface. System outflows in the model are discharge to the stream and ET. Recharge is assumed to be the only inflow to the system. The mass balance approach for our hypothesis consists of a steady state balance where inflows are equal to outflows. This mass balance is derived as follows

$$(Q_{IN} + Q_R) - Q_{OUT} = Q_{ET}$$

if due to the divide $Q_{IN} = 0$

$$Q_R - Q_{OUT} = Q_{ET} \qquad (1)$$

Then the mass balance is given by

$$C_R Q_R = C_{OUT} Q_{OUT} + C_{ET} Q_{ET}$$

as $C_{ET} = 0$, then

$$C_R Q_R = C_{OUT} Q_{OUT}$$

rearranging

$$\frac{Q_R C_R}{C_{OUT}} = Q_{OUT} \qquad (2)$$

Combining (1) and (2)

$$Q_R - \left(\frac{C_R}{C_{OUT}} Q_R \right) = Q_{ET} \qquad (3)$$

the evapotranspiration flow is then given by and

$$Q_{ET} = Q_R \left(1 - \frac{C_R}{C_{OUT}} \right) \text{ , and}$$

$$\frac{Q_{ET}}{Q_R} = 1 - \frac{C_R}{C_{OUT}} \qquad (4)$$

Where Q_{OUT} is the flow leaving the aquifer into the river, Q_{ET} is the flow leaving the aquifer by evapotranspiration, Q_R is the flow entering the aquifer by recharge, Q_{IN} is the flow entering the aquifer, C_{OUT} is the conductivity of water going into the river and C_R is the conductivity of the recharge water. Figure 2 represents the geometry of the mass balance.

The conductivity is assumed to be linearly proportional to solute concentration, therefore it can be used in the mass-balance expression

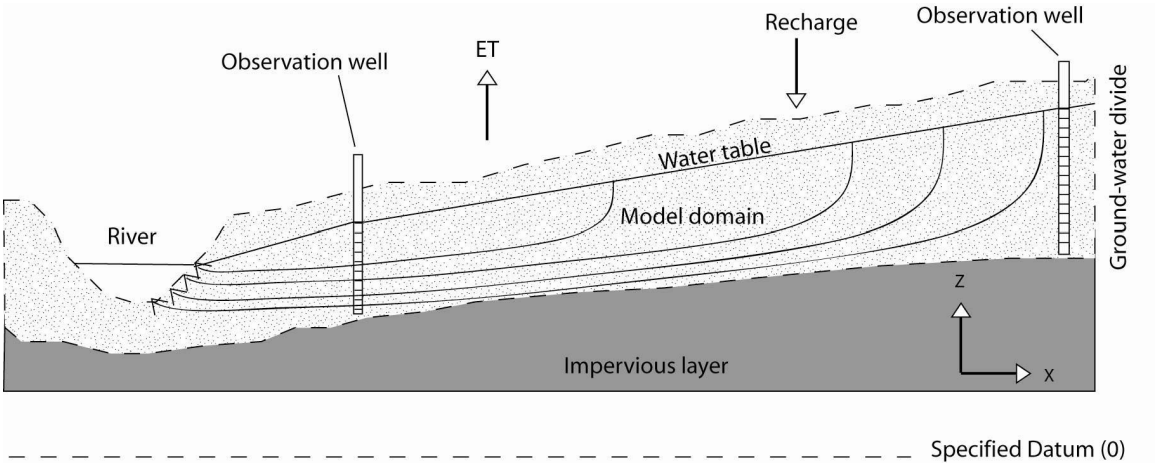

Fig. 1. Aquifer geometry (adapted from Thompson 2003).

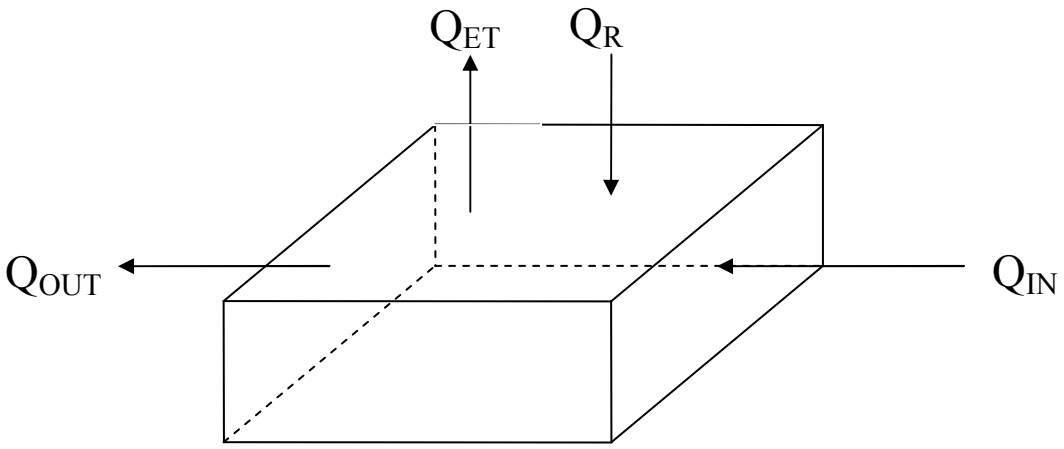

Fig. 2. Aquifer mass balance geometry, where inflows, Q_{IN} and $Q_{R,}$ are equal to outflows, $Q_{OUT,}$ Q_{ET}.

3. Methods

3.1 Data Acquisition

Pringle Branch basin is the field site chosen for this study. It is a small second-order basin located in southeast Hillsborough County, Florida. The field site has a contributing drainage basin area of approximately 12 km^2 (Fig. 3). The profile extends 400 meters from the divide to the stream. The land cover is unimproved grass pasture on the upper slope and riparian woodlands within 100-150 m of the stream. The main canopy of the riparian wetland is comprised of lush hardwoods and the understory is comprised of palms and mixed, dense ground cover. The stratigraphy consists of shallow sediments of 2 to 3 m of very fine sand over silts and clays followed at depth by a sandy, silty, clay layer that acts as the lower boundary of the shallow aquifer. This shallow aquifer is part of the Surficial Aquifer system.

The field study consisted of seven months of data collection during which weekly head levels and ground-water conductivity measurements were collected. Runoff and near surface interflow water and terrain conductivity were also measured. Parameters such as hydraulic conductivity, porosity and specific yield were taken from previous studies (Thompson, 2003; Schwartz & Zhang, 2003). ET data were provided by Tampa Bay Water (TBW).

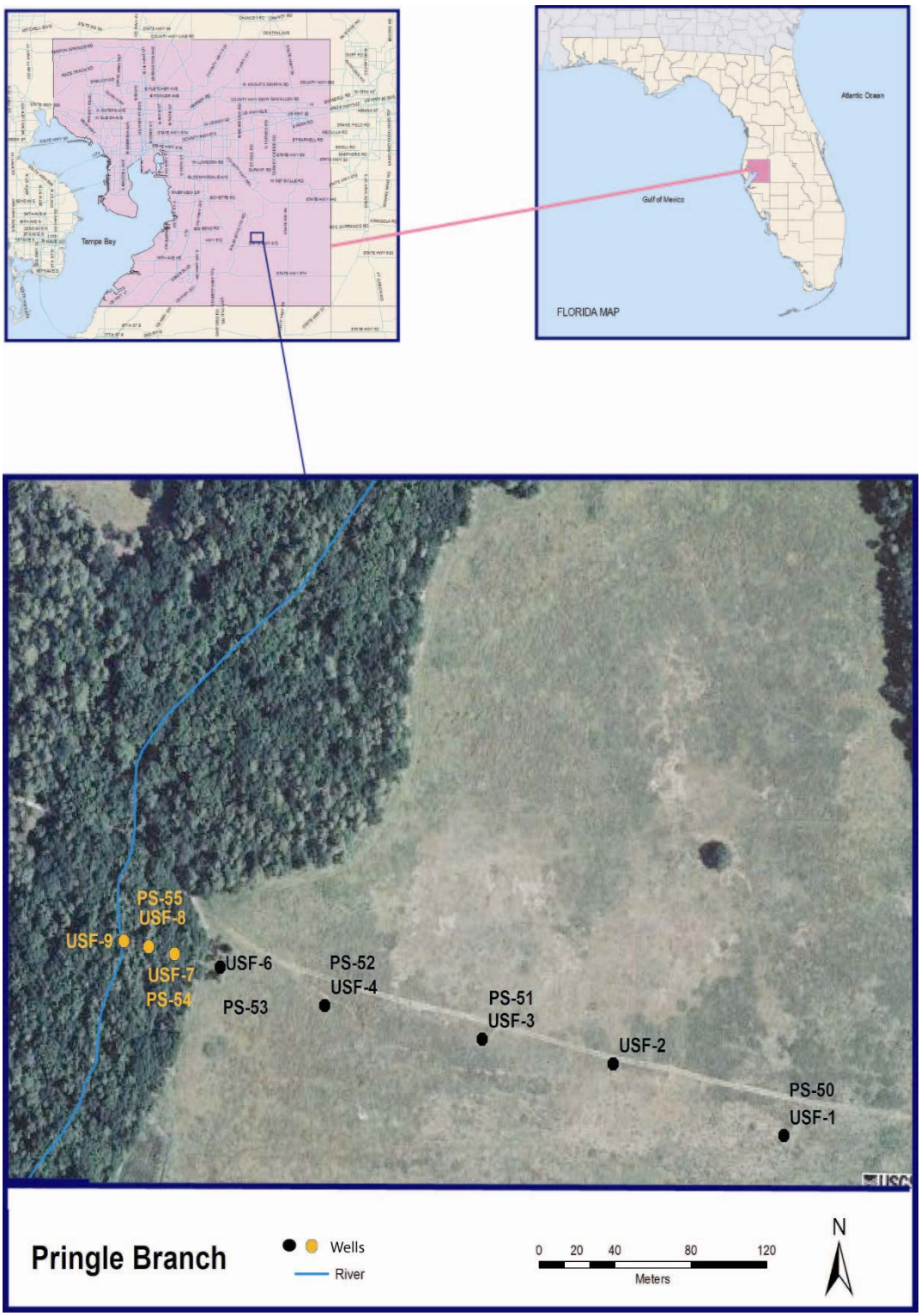

Fig. 3. Pringle Branch location

3.1.1. Well installation

Several wells were installed along a profile from divide to stream using drive-point piezometers, with 2 cm diameter by 15 cm long well points (USF wells, Fig. 3). Each well nest has a shallow well placed 25 cm below water-table and a deep well, 1 m below shallow wells (Fig. 4). The wells were developed to remove fine particles and permit representative water sampling. In addition, shallow wells maintained by TBW (PS wells, Fig. 3), were also sampled and measured. These wells are approximately 6 m deep, with 3 m screen (HDR, 2000).

3.1.2. Water conductivity.

Ground-water conductivity measurements were obtained in the field with a portable conductivity meter. Each water sample was taken after pumping three times the well volume. At some times during the study, some wells did not have enough water to pump three times their volume and some wells went dry. Measurements were taken when less than three well volumes were pumped, but were noted in the field notes.

A runoff sampling station was set up to collect surface runoff and near-surface interflow during storm events. R. Degraaf carried out a soil-water experiment where water conductivities due to water-soil interaction were measured (unpublished data). Rainwater collected at the site was placed in containers with soil samples taken from different depths at the site. The samples were agitated daily and fluid conductivities measured at intervals for 14 days.

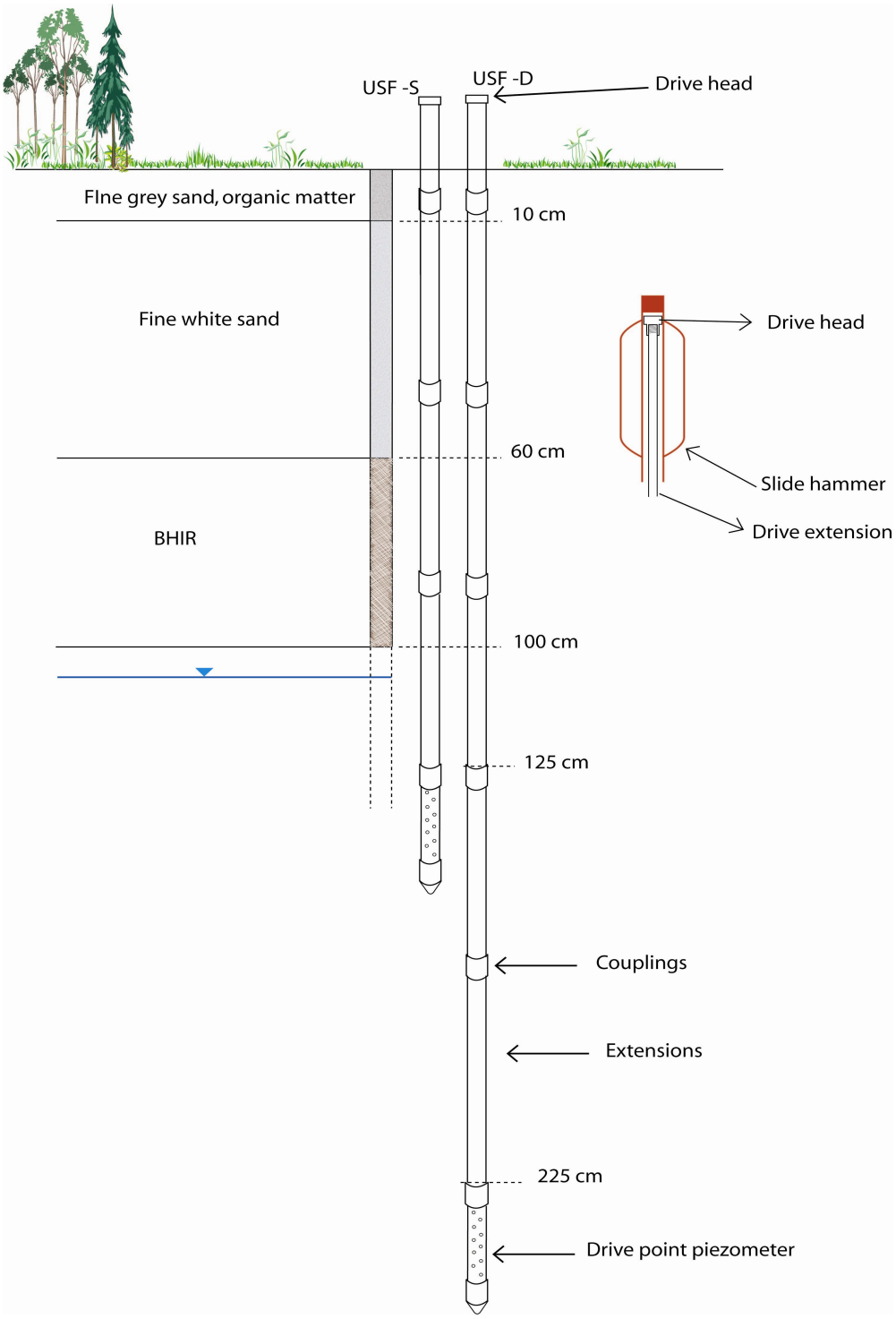

Fig. 4. Sketch of the well nest, with a shallow and deep well, installed for this project with a slide hammer

3.1.3. ET data

TBW has a weather station at the divide at 5 m north from the USF-1 well. Precipitation and pan evaporation rates (ET_{pan}) were taken from that station. The potential evaporation rates come from a standard evaporation pan (Chin & Zhao, 1995). Actual data for the site were obtained from TBW.

ET_{pan} data were used only to calculate the correlation with ground-water conductivity. The average ET rates introduced in the numerical model are not calculated from pan evaporation, but were obtained from soil moisture measurements using time-domain reflectometry (Nachabe et al. 2005).

3.1.4. Geophysics.

Terrain conductivity was measured with an electromagnetic technique, a Geonics EM 31 (Geonics, 1995). Terrain conductivity is determined principally by porosity and fluid conductivity. The instrument was operated in vertical dipole mode, at 1m height over the land surface. Two surveys, following the same survey lines, were completed on different dates, once during the dry season and once during the wet season. Terrain conductivity values were obtained along the well profile and on to parallel lines 50 m on either side of the well profile. Measurements were taken every 10 meters along the lines (Fig. 5).

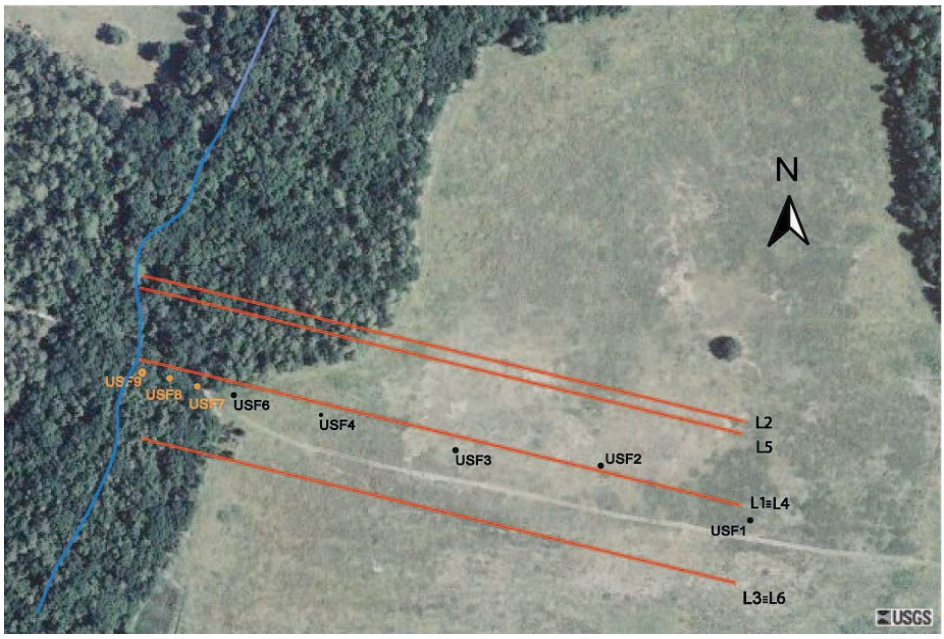

Fig. 5. EM31 survey grid. L1 and L4 lines are along the profile. L1, L2 and L3 were taken in March 2005; L4, L5, L6 were taken in May 2006.

3.2. Mass-transport model.

To test the hypothesis that the principal influence on ground-water conductivity is ET, a mass-transport, numerical ground-water model was constructed that uses observed values of ET and basin parameters. The model-predicted ground-water conductivity was compared to observed values to estimate the influence of ET on ground-water conductivity.

The mass-transport in the aquifer is governed by an advection-dispersion equation, assuming isotropic and homogeneous conditions (Stewart et al. 2006). This mathematical model is solved setting up a finite-difference model that uses the MODFLOW and MT3D codes (McDonald & Harbaugh, 1984; Zheng, 1990)

The finite-difference model consists of a vertical-profile model where no-flow cells define the geometry of the aquifer. In a simple approach, only four layers are used to define the model (Fig. 6). The grid consists of 1 row, 40 columns and 4 layers, a total of 160 cells from which 112 are actives. Each cell has dimensions 10 m long, 5 m wide and 2.25 m deep.

Boundary conditions are no-flow boundary cells in the bottom boundary, a river cell for the outflow and three constant head and concentration cells at the right side of the model.

Hydraulic conductivity is 5m/d (Thompson, 2003), and porosity and specific yield are respectively 0.35 and 0.3 (Schwartz & Zhang, 2003).

Two different values of ET and recharge are introduced in the model representing the two different vegetation zones. They use the same zonation, one zone for the grass on the upper slope and one zone for the riparian woodlands in the woodland area, ET is approximately 146 cm per year and in the grass area, ET is 73 cm per year, as determined from soil moisture measurements (Nachabe et al. 2005). To provide a nearly constant modeled ET rate with vertical variations in water-table elevation, large values were used for the MODFLOW ET extinction depth, 6m for grass and 18 m for the forest area. Recharge was determined as a calibration parameter in the model.

The conductivities introduced in the mass-transport model are the recharge conductivity, 25 uS/cm (average rain conductivity) and the initial concentration of the aquifer, 90 uS/cm (maximum soil-water interaction conductivity). The ET concentration is assumed to be 0. Average concentration values from Stewart et al. 2006 are used to

calibrate the mass transport model (Fig.7). Wells used in Stewart et al. 2006 are the PS series wells.

The longitudinal dispersivity coefficient introduced in the model is 10m, or about 4% of the total flow distance. This value was chosen to minimize the mass-balance error in the mass-transport model. The flow model does not simulate sorption or dissolution, as it is assumed that the principal ions that contribute to fluid conductivity are geochemically conservative and are provided by recharge and initial recharge/soil interactions.

A dynamic steady-state solution was achieved by using a transient model with a very long total simulation to insure that steady-state conditions were achieved. The final model was run for 50,000 days, using 10 time steps in the flow model and 133 transport steps in the mass transport.

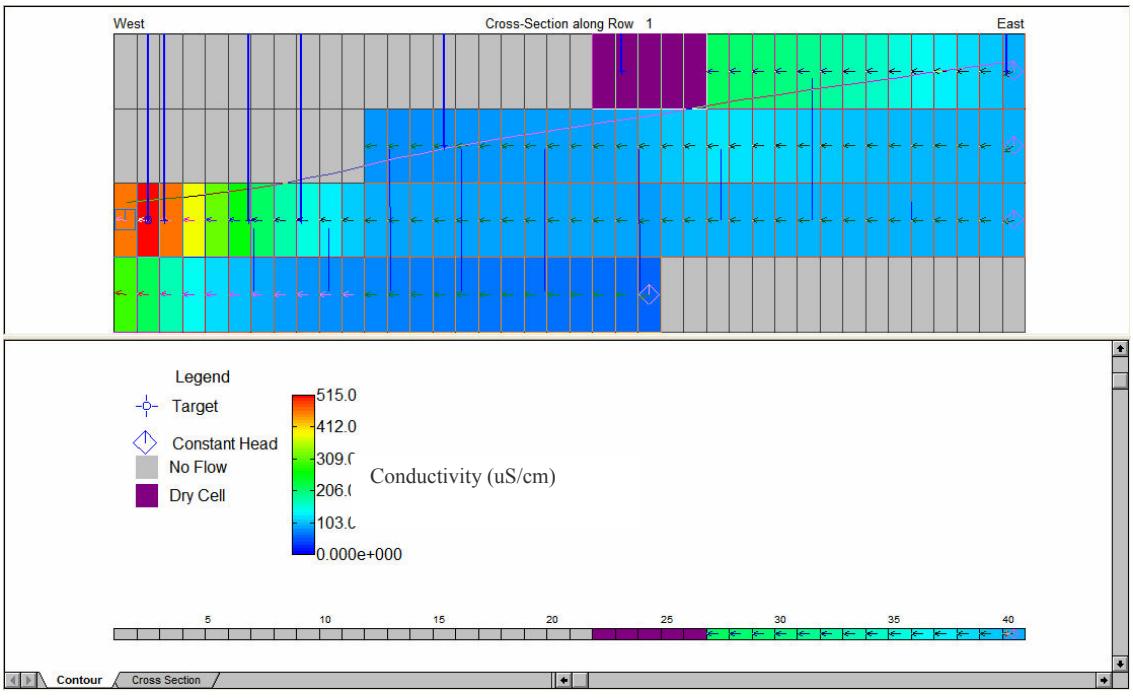

Fig. 6. Numerical model sketch.

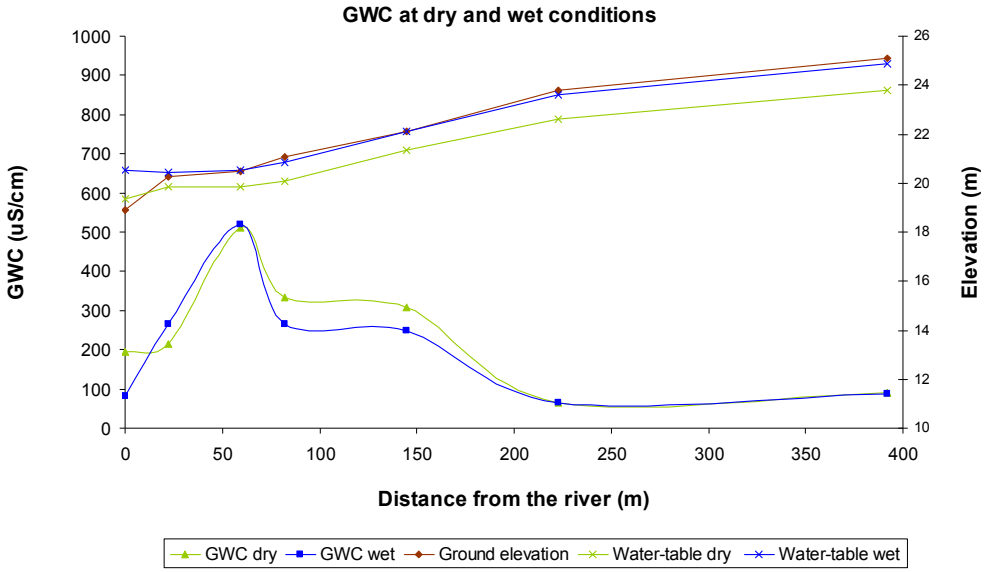

Fig. 7. Ground-water conductivity (GWC) data taken from Stewart et al. 2006. Measurement points are PS wells. High ground-water conductivity values are located in the wooded area. These data were used as input data in the numerical model.

4. Results

4.1. Field data.

The soil-water experiment conducted by R. Degraaf (unpublished data) gives the maximum value of conductivity that can be reached by soil-water interaction, 90uS/cm (Fig. 8). After 7 days, the soil sample from the land surface produced the highest fluid conductivity, 90 uS/cm.

As the water table is near land surface, ground-water conductivity should have a significant influence on terrain conductivity. Comparing terrain-conductivity data to ground-water conductivity it can be seen that both have the same spatial behavior but absolute values of terrain conductivity data are lower (Fig. 9), as would be expected as terrain conductivity includes both fluid and matrix conductivity. The fact that each terrain-conductivity survey line shows the same conductivity pattern supports the assumption that the two dimensional numerical model is a reasonable conceptual model.

Over seven months of weekly measurements the pattern of fluid conductivity initially found in the basin is essentially maintained for the entire monitoring period, from dry to wet season (Fig. 10). Ground-water conductivity increases moderately from the divide to the stream, and then increases prominently where the change in vegetation to riparian woodland occurs. Changes in ground-water conductivity values at individual wells with time generally are not greater than 40% (Fig. 10). Although at USF-2 the change is greater than 40%, the values at this well may be suspect because the well

became dry on 2/6/2006 and did not refill until 7/6/2006. In order to see if the changes on ground-water conductivity with time are related to ET, both datasets were compared.

ET_{pan} values were compared with ground-water conductivity values at USF-1 deep. The selection of this well is because it is the closest well to the weather station where the ET_{pan} data come from. The correlation coefficient between ground-water conductivity and ET_{pan} is 0.55 and the p value 0.0024 (Fig. 11). Thus, ground-water conductivity is positively correlated with respect to ET_{pan} at the 95% confidence level. The cross correlation shows no lag time between both time series (Fig. 12).

Recharge can also influence in changes in ground-water conductivity. Making a balance between ET and precipitation values (ET-P) and comparing it with ground-water conductivity the correlation coefficient increases to 0.56.

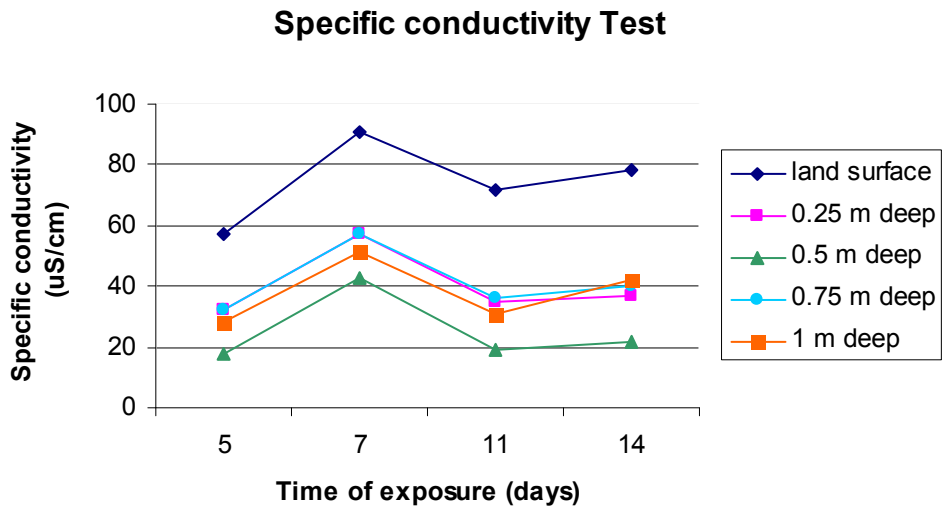

Fig. 8. Specific conductivity test with soil samples from different depths, land surface, 0.25m, 0.5m, 0.75m and 1m.

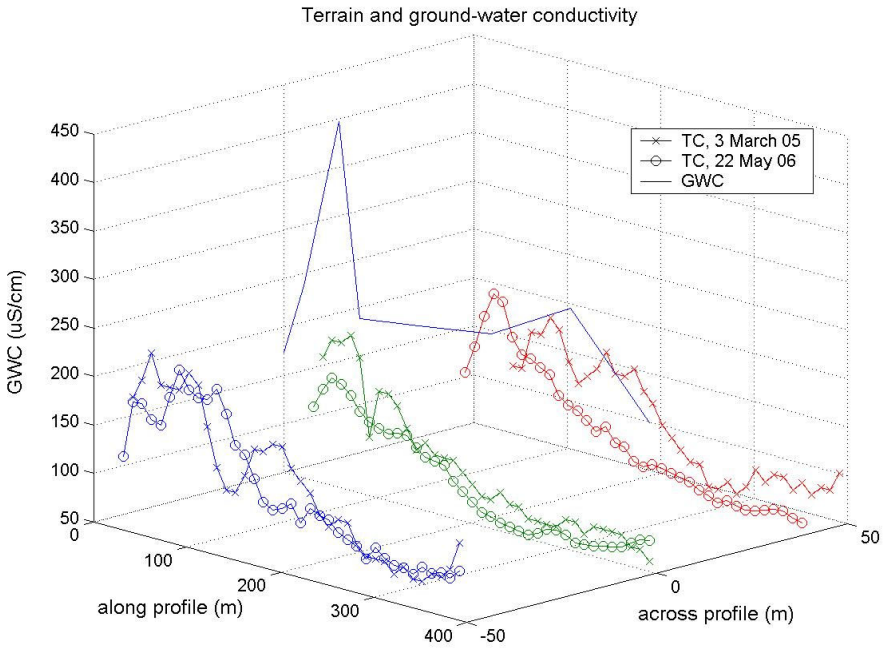

Fig. 9. Terrain-conductivity (TC) data taken with EM-31 in March 05 and May 06, at different parallel lines of the aquifer profile. Ground-water conductivity (GWC) values are average values of deep USF wells.

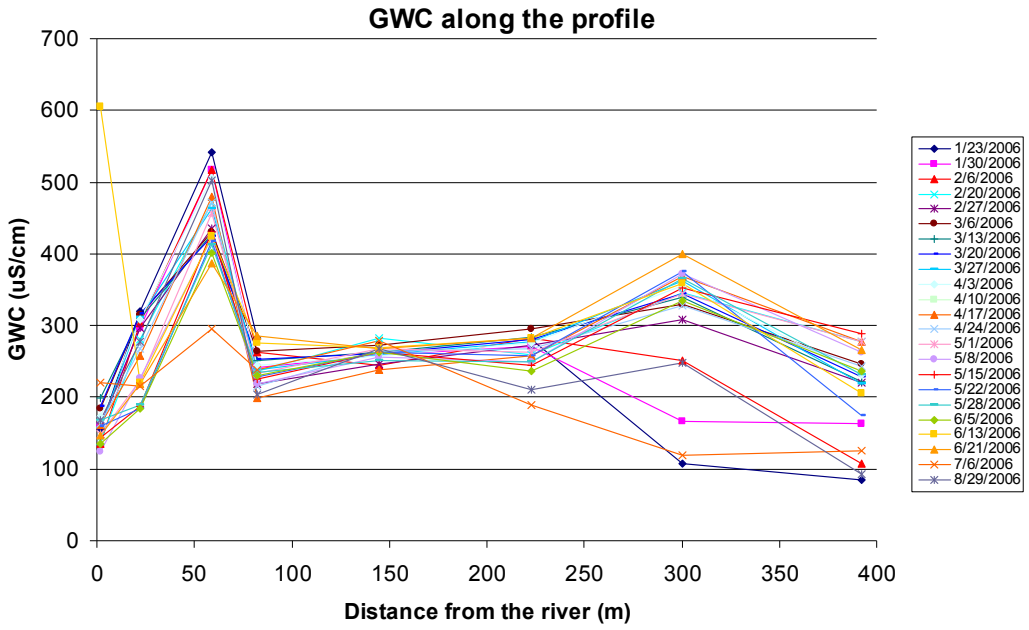

Fig.10. Ground-water conductivity values along the profile. Each line represents a different sampling time. Values are from USF deep wells.

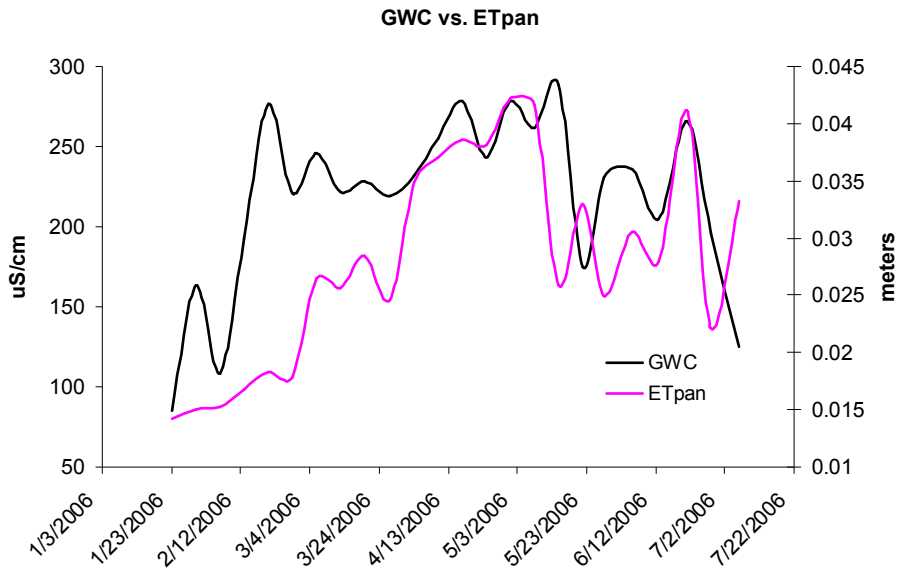

Fig. 11. Weekly average ET_{pan} data versus ground-water conductivity (GWC). The correlation coefficient is 0.55 and the p value 0.0024.

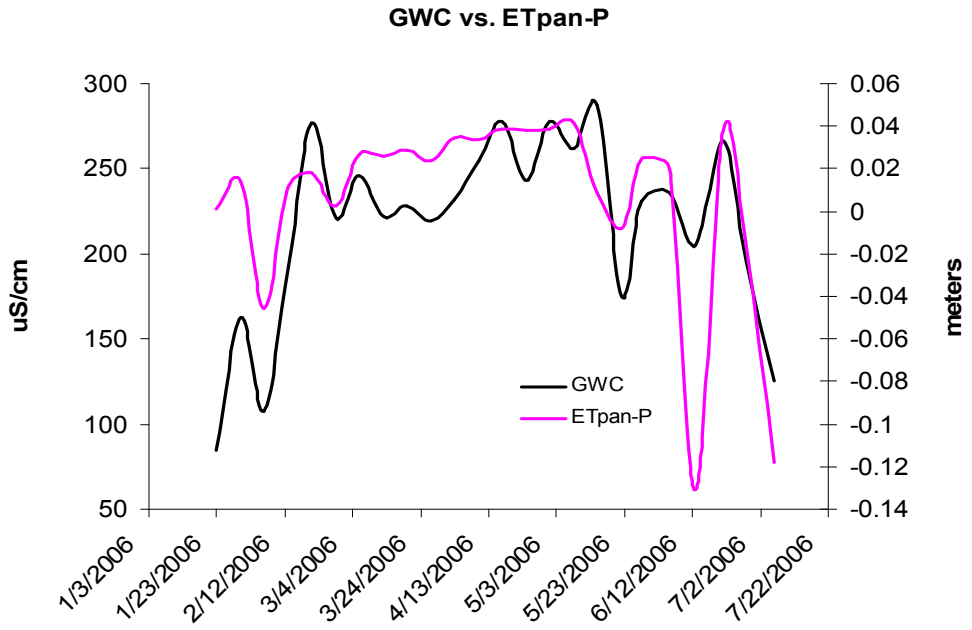

Fig. 12. Ground-water conductivity versus weekly average balance between ET_{pan} and precipitation data. The correlation coefficient is 0.56 and the p value 0.0021.

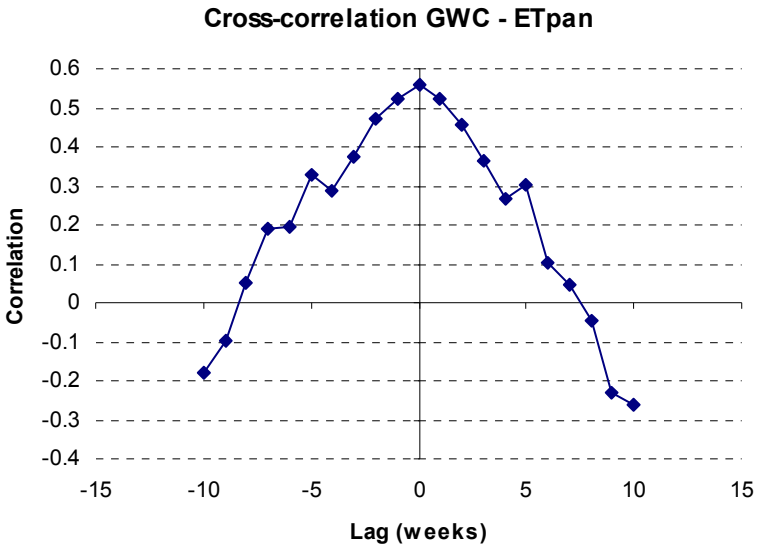

Fig. 13. Cross Correlation between ET_{pan} and ground-water conductivity. There is no lag time between both datasets for weekly measurements.

4.2. Numerical model

The flow model, MODFLOW, uses steady-state conditions in a transient model, while the mass-transport model is run as transient with constant stresses. The mass-transport model simulation times are long enough to reach stable concentrations. After a period of approximately 19 years the flow model reaches the steady-state condition. The mass-transport model reaches the steady state at 34 years of simulation time (Fig.14).

The calibrated values of recharge are 0.13 and 9E-07 cm/d in the grass and forest area respectively. The flow-model mass balance error is 0.03% and the transport model mass balance error is 9.8%. Residual values between calculated and observed data in the flow model are lower than in the transport model (Table 1).

The results from the numerical model show that introducing two different values of ET and recharge for the two different types of vegetation creates a concentration pattern along the profile similar to the one observed in the field (Fig. 15). Although the pattern is similar, modeled ground-water conductivity has higher values close to the stream than the field values.

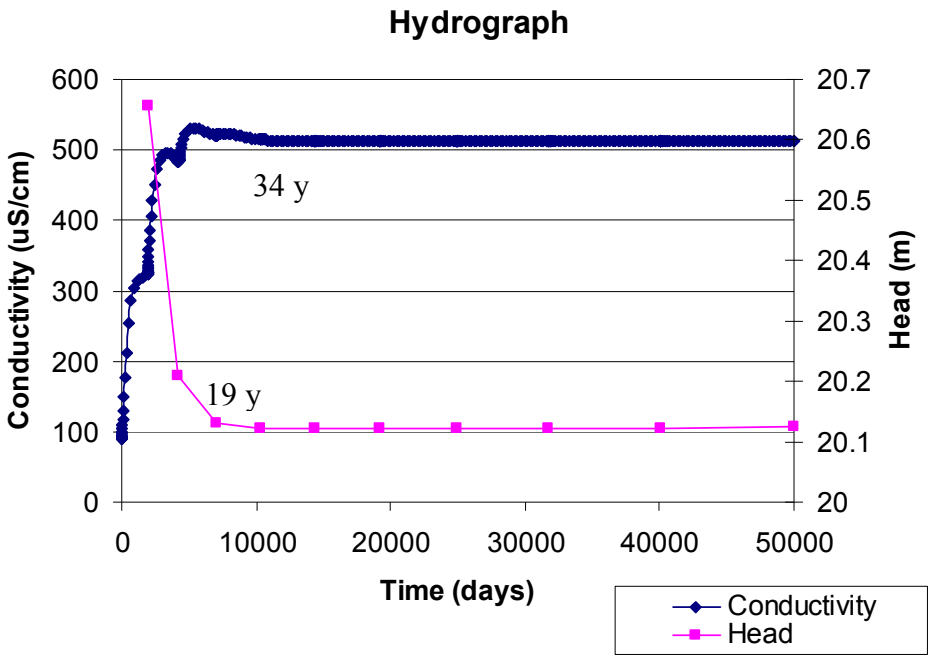

Fig. 14. Change of head and conductivity in a monitor well at 15m from the stream. Times at which the models reach the steady state can be seen.

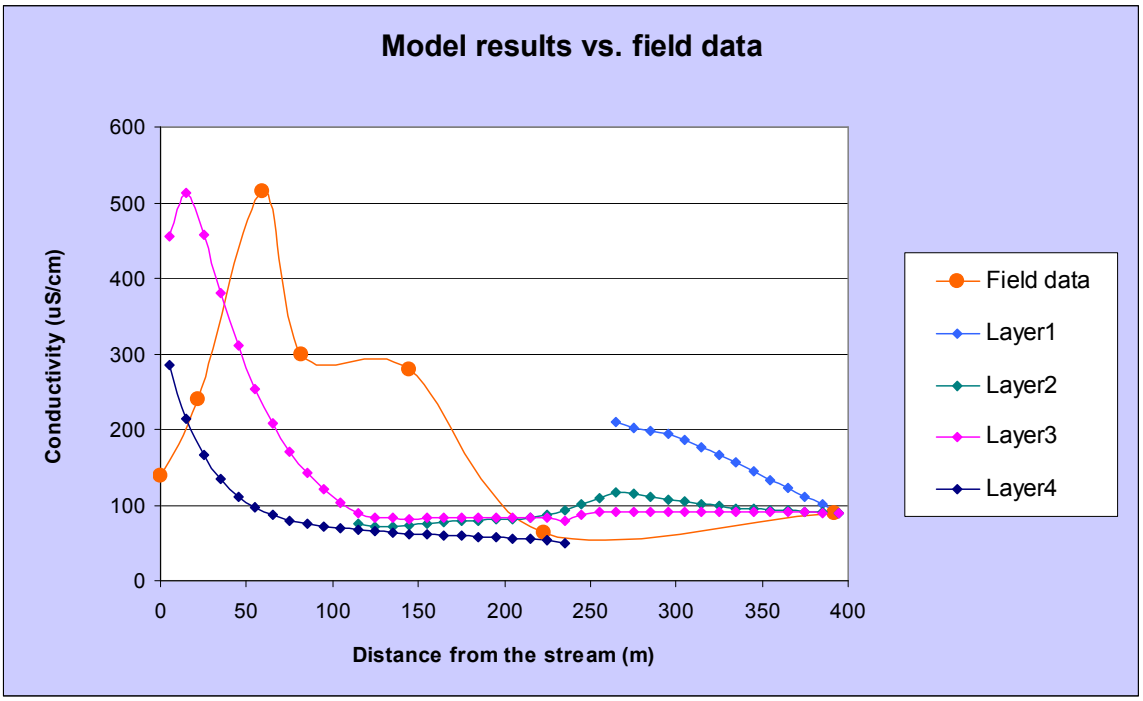

Fig. 15. Results from the numerical model. Note that layer 3 shows a peak on conductivity similar to the one observed in the field.

	Flow model			Transport model		
Target	Target value	Model value	Residual (m)	Target value	Model value	Residual (uS/cm)
PS-51	19.94	20.1824	-0.2424	64	-1	65
PS-52	20.19	20.4354	-0.2454	286	72.7315	213.2685
PS-53	20.47	20.7923	-0.3223	304	143.254	160.746
PS-54	21.72	21.6833	0.0367	515	253.692	261.308
PS-55	23.1	22.9	0.2	233	458.445	-225.445

Table 1. Residual values from the numerical model. -1 in conductivity means that the cell was dry.

5. Discussion.

Looking at the results from the soil-water conductivity test, it can be seen that the highest conductivity values obtained from soil-water interactions are low compared to the highest ground-water conductivities, 90 uS/cm compared to 500 uS/cm. This suggests that the higher values of ground-water conductivities observed in the field can not be achieved by soil-water interactions.

As suggested by the results from the numerical model, two different ET and recharge values are enough to reproduce the general conductivity pattern observed in the field. The two recharge values used in the model correspond to low recharge in the forest area where the water-table is at or near the land surface for a long period of time. During that time, little or no recharge can go into the system. Thus, the annual recharge value in the riparian woodlands can be assumed to be lower than in the grass, where the water-table is deeper (Stewart et al., 2006).

The extinction-depth values used in the MODFLOW ET package are greater than the actual extinction depth in the field. The ET package in MODFLOW does not take into account transpiration from plants and the unsaturated zone, and treats ET as a linear relationship between the maximum evaporation at the land surface and zero evaporation at the stated extinction depth (Fig. 16) (Baird & Maddock, 2005). For this reason, the average ET calculated by MODFLOW is lower than field observations for equivalent extinction depths. Using deeper extinction depths decreases the decrease in modeled ET

with depth when the water-table is below land surface. This results in a more uniform ET rate for small variations in water-table depth. Increasing the extinction depth in MODFLOW increases the average ET in the model, allowing a better match between measured ET and the MODFLOW results.

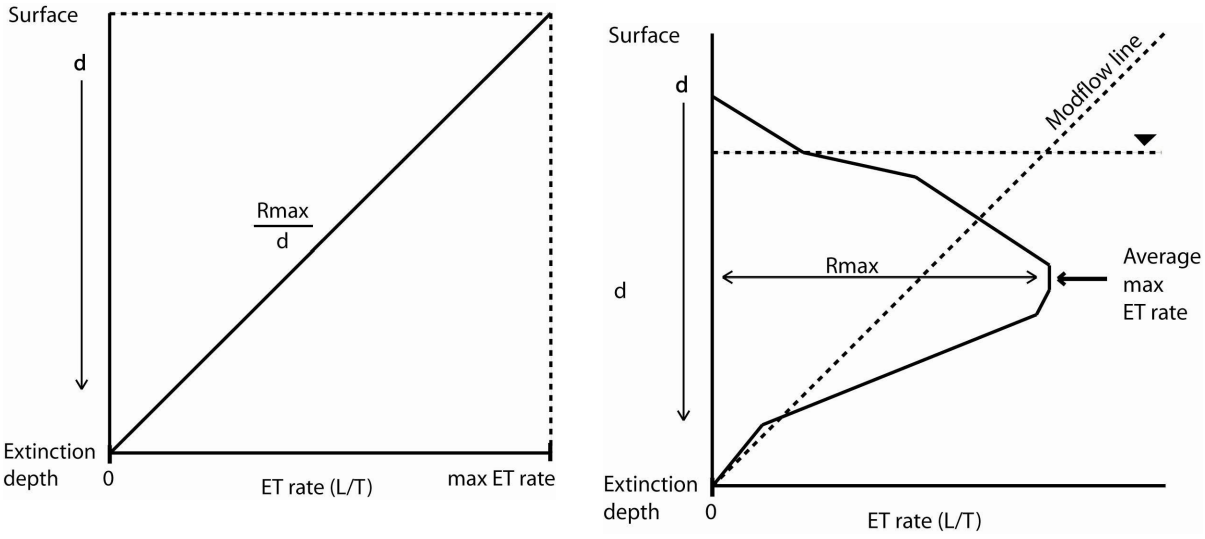

Fig. 16. Different approaches to calculate ET. MODFLOW approach on the left and more realistic approach on the right (from Baird & Maddock, 2005)

Ionic fractionation when water is taken up by plants is negligible. However, the system is assumed to be in a long-term equilibrium, in that it is assumed that the minerals taken up by the plants at the roots are returned to the soil once the plant materials die and decompose. Therefore, in a long-term equilibrium, ET has conductivity 0, as water transpired at the leaves has a TDS of 0.

The peak conductivity value in the model has the same conductivity value as the field data, but is not in the same place as the field peak (Fig. 15). The modeled peak

conductivity is closer to the stream than the observed data This displacement of the modeled conductivity could be related to the aquifer-river interactions that are not included in the model, such as flooding. The model results also show a sharp discontinuity in conductivity from layer to layer. These discontinuities can be explained by the relatively coarse vertical discretization of the model.

6. Conclusions.

The field data suggest that ground-water conductivity is strongly related to evapotranspiration processes. The overall pattern followed by ground-water conductivity along the profile appears to be driven by spatial variations in ET more than time variations or interaction with the aquifer matrix. Small changes in ground-water conductivity can be explained by changes in ET with time. Weekly changes in shallow ground-water conductivity are strongly correlated with ET_{pan} rates. The 40% variation in ground-water conductivity values over the 7-month sampling period can be attributed to short-term variations in ET_{pan}.

The mass-transport model was designed to test the hypothesis that ground-water conductivity is controlled principally by ET. The model results confirm the hypothesis that ground-water conductivity is principally influenced by ET. This suggests that patterns of ground-water conductivity measured by direct sampling or terrain conductivity surveys can be used to estimate ET rates and spatial variations in ET rates in small basins.

Because MODFLOW does not treat ET in a realistic way, the numerical model results in this study are strictly valid only as a test of the hypothesis. The numerical model used on this study suggests that ET is the principal determinant of ground-water conductivity in a small basin. The results suggest that the role of ET in determining

ground-water conductivity should be further investigated with a model capable of better simulating ET from both above and below the water table.

7. References

Allen, R.G., Jensen M.E., Wright, J.L., Burman, R.D. (1989). *Operational estimates of evapotranspiration*. Agronomy Journal 81, 650-662.

Anderson, M.P., Woessner, W.W. (2002). *Applied groundwater modeling: simulation of flow and advective transport*. Elsevier Ed.

Baird, K., Maddock, T. (2005). *Simulating riparian evapotranspiration: a new methology and application for groundwater models*. Journal of Hydrology 312, 176-190.

Bauer, P., Thabeng, G., Stauffer, F., Kinzelbach, W. (2004). *Estimation of the evapotranspiration rate from diurnal groundwater level fluctuations in the Okavango Delta, Botswana*. Journal of Hydrology 288, 344-355.

Bowen, I.S. (1926). *The ration of heat losses by conduction and by evaporation from any water surface*. Physical Review 27, 779-787.

Chen, X., Chen, X. (2003). *Stream water infiltration, bank storage zone changes due to stream-stage fluctuations*. Journal of Hydrology 280, 246-264.

Chin, D., Zhao, S. (1995). *Evaluation of evaporation-pan networks.* Journal of Irrigation and Drainage Engineering, Vol. 121, n 5, 336-348.

Cimino, J.A. (2003). *Empirical mass balance calibration of analytical hydrograph separation techniques using electrical conductivity*. M.S. Thesis. University of South Florida.

Dolan, T.S., Hermann, A.J., Bayley, S.E., Zoltek, J. (1984). *Evapotranspiration of Florida U.S.A., freshwater wetland*. Journal of Hydrology 74, 355-371.

Kite, G.W. (2000). *Using a basin-scale hydrological model to estimate crop transpiration and soil evaporation*. Journal of Hydrology 229(1-2), 59-69.

Kite, G.W., Droogers, P. (2000). *Comparing evapotranspiration estimates from satellites, hydrological models and field data*. Journal of Hydrology 229, 3-18.

Laudon, H., Slaymaker, O. (1997). *Hydrograph separation using stable isotopes, silica and electrical conductivity.* Journal of Hydrology 201, 82-101.

Lund, M.R., Soegaard, H. (2003). *Modelling of evapotranspiration in a sparse millet crop using a two-source model including sensible heat advection within the canopy*. Journal of Hydrology 280, 124-144.

Mao, L.M., Bergman, M.J., Tai, C.C. (2002). *Evapotranspiration measurement and estimation of three wetland environments in the upper St. Johns River Basin, Florida*. Journal of the American Water Resources Association Vol. 38 n. 5, 1271-1285.

McDonald, M.G., and Harbaugh, A.W., (1984*) A modular three-dimensional finite-difference ground-water flow model*: U.S. Geological Survey Open-File Report 83-875, 528 p.

Nachabe, M., Shah, N., Ross, M., Vomacka, J. (2005). *Evapotranspiration of two vegetation covers in a shallow water table environment.* Soil Science Society of America Journal Vol. 69, 492-499.

O'Brien, C., Hendershot, W.H. (1993). *Separating streamflow into groundwater, solum and upwelling flow and its implications for hydrochemical modelling*. Journal of Hydrology, 146 1-12.

Penman, H.L. (1948). *Natural evaporation from open water, bares, soil and grass*. Royal Soc., London Proc. Ser. A. 193, 120-146.

Rein, A., Hoffman, R., Dietrich, P. (2004). *Influence of natural time-dependent variations of electrical conductivity on DC resistivity measurements*. Journal of Hydrology 285, 215-232.

Roerink, G.J., Su, Z., Menenti, M. (2000). *S-SEBI: a simple remote sensing algorithm to estimate the surface energy balance*. Physics and Chemistry of the Earth, Part B 25 (2), 147-157.

Rosenberry, D.O., Winter, T.C. (1997). *Dynamics of water table fluctuations in an upland between two prairie-pothole wetlands*. Journal of Hydrology 191, 266-289.

Schwartz, F.W., Zhang, H. (2003). *Fundamentals of Ground Water*. John Wiley & Sons, Inc.

Stewart, M., Cimino J., Ross M. (2006). *Calibration of baseflow separation methods with streamflow conductivities*. Ground Water.

Swinbank, W.C. (1951). *The measurement of vertical transfer of heat and water vapour by eddies in the lower atmosphere*. Journal of Meteorology 8, 135-145.

Thompson, D.L. (2003). *Specific yield variability and the evolution of ground-water evapotranspiration in a humid shallow water table environment*. M.S. Thesis. University of South Florida.

Vacher, H.L., Ayers, J.F. (1980). *Hydrology of small oceanic islands. Utility of an estimate of recharge inferred from chloride content of fresh-water lenses*. Journal of Hydrology 45, 21-37.

Wittenberg, H., Sivapalan, M. (1999). *Watershed groundwater balance estimation using streamflow recession analysis and baseflow separation*. Journal of Hydrology 219, 20-33.

Yoshimasa, F., Fahey, M., Newson, T. (2000). *Field investigation of evaporation from fresh tailings*. Journal of Geotechnical and Geoenvironmental Engineering, Vol. 126, No.6, 556-567.

Zheng, C., (1990). MT3D*, A modular three-dimensional transport model for simulation of advection, dispersion and chemical reactions of contaminants in groundwater systems*. Report to the U.S. Environmental Protection Agency, Robert S. Kerr Environmental Research Laboratory, Ada, OK.

Zheng, C., Bennett, G. (1995). *Applied contaminant transport modeling: theory and practice*. Van Nostrand Reinhold, A Division of International Thompson Publishing Inc.

Geonics Limited (1995). *EM31-MK2 Operating manual*.

HDR Engineering, Inc. (2000). *Tampa Bay Regional Reservoir. Reservoir Seepage Evaluation.*

Appendices

Appendix A. Soil analysis example

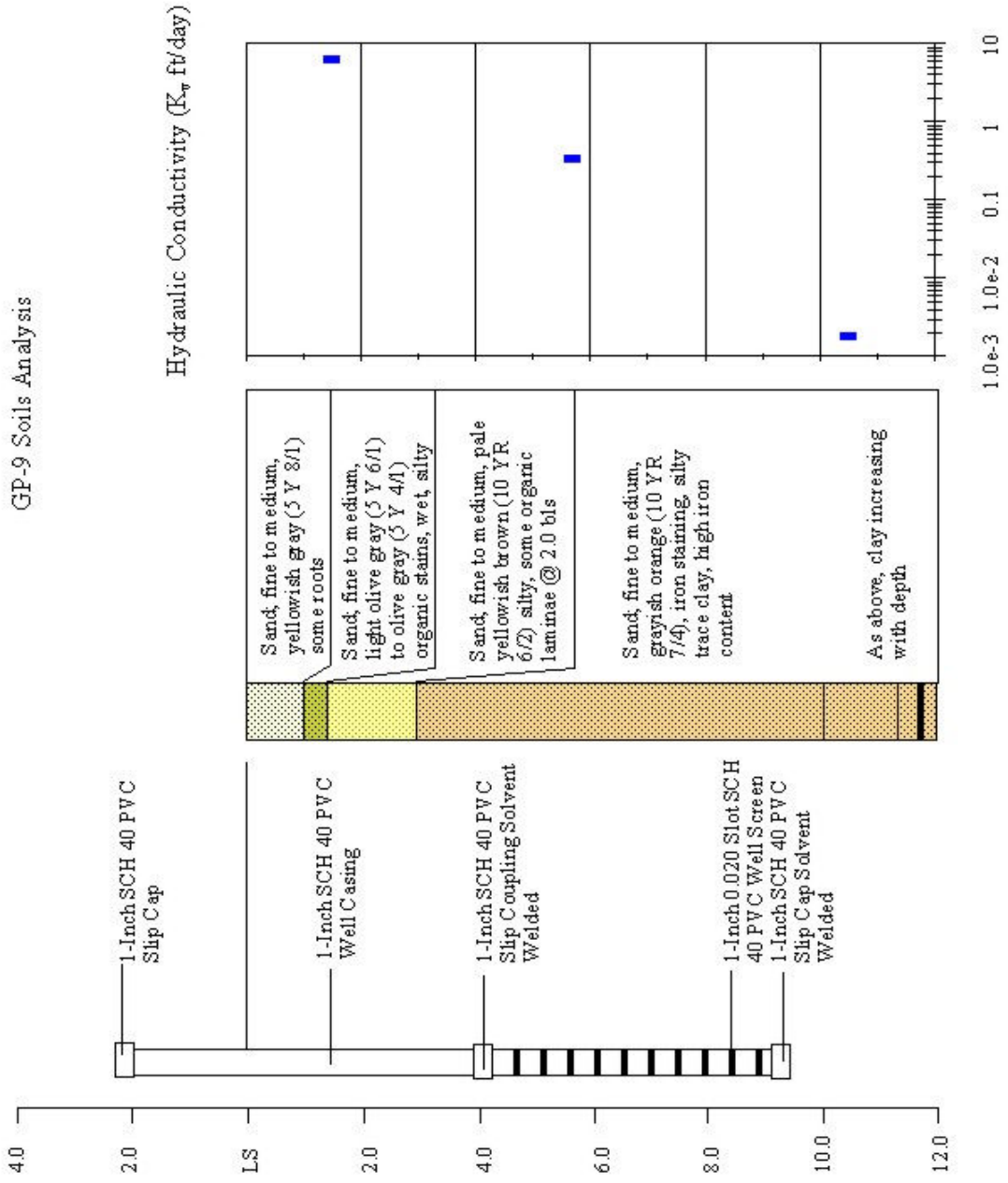

Fig. 17. Example of soil analysis from Thompson, 2003. They were used to calculate the depth of the impermeable layer. Well GP-9 corresponds to PS-51 in our study

Appendix B. Equipment

The instrument used to measure the electric conductivity of the water is a conductivity meter ExStik EC400. Its accuracy is ± 2% full scale and has a conductivity range of

0 to 199.9µS/cm
200 to 1999µS/cm
2.00 to 19.99mS/cm

Fig. 18. Conductivity meter device

The test sample is placed in a sample cup with depth 2.5cm minimum to cover the electrode. The solution is stirred to remove any air bubbles and the conductivity meter is introduced to measure the conductivity.

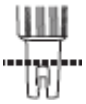

Appendix C. Data

Well ID	Distance from stream (m)	Surface elevation (m)	Dry conditions WT elevation	Conductivity (uS/cm)	Wet conditions WT elevation	Conductivity (uS/cm)	Average WT elevation (m)	Average conductivity (uS/cm)
50	392	25.09	23.8	90	24.87	87	24.335	88.5
51	223	23.77	22.62	64	23.59	64	23.105	64
52	145	22.13	21.34	308	22.1	249	21.72	278.5
53	82	21.06	20.09	332	20.85	265	20.47	298.5
54	59	20.48	19.87	511	20.51	520	20.19	515.5
55	22	20.27	19.84	215	20.42	265	20.13	240
Stream	0	18.9	19.35	194	20.54	83	19.945	138.5

Table 2. Elevations and conductivities used as targets in the model. (Stewart et al. 2006)

Date	GWC	ET(m)	Precipitation (m)
1/23/2006	85	0.014224	0.013208
1/30/2006	163	0.014986	0.00127
2/6/2006	108	0.01524	0.060706
2/13/2006	192.5	0.016764	0.00508
2/20/2006	277	0.018288	0
2/27/2006	221	0.01778	0.015494
3/6/2006	246	0.026416	0
3/13/2006	222	0.025654	0
3/20/2006	228	0.028448	0
3/27/2006	219	0.024638	0.000762
4/3/2006	232	0.034798	0
4/10/2006	255	0.037084	0.003556
4/17/2006	278	0.038608	0
4/24/2006	243	0.0381	0
5/1/2006	278	0.042164	0.003302
5/8/2006	262	0.041656	0
5/15/2006	288	0.025908	0.017018
5/22/2006	175	0.03302	0.041402
5/28/2006	231	0.024892	0.000254
6/5/2006	236	0.03048	0.010414
6/13/2006	205	0.02794	0.15875
6/21/2006	266	0.041148	0.002794
6/28/2006	195.5	0.022098	0.038862
7/6/2006	125	0.033274	0.151638

Table 3. Ground-water conductivity (from USF-1), ET and precipitation data used in the correlations.

Table 4. Head elevation data (m)

	USF-1D	USF-2D	USF-3D	USF-4D	USF-6D	USF-7D	USF-8D	USF-9D	PS-51	PS-53
1/23/2006	23.76	22.80	22.25	20.97	20.26	20.04	20.02	20.02	22.35	20.24
1/30/2006	23.65	22.72	22.30	21.04	20.14	19.95	19.94	19.96	22.60	20.15
2/6/2006	24.05	23.04	22.66	21.24	20.81	20.35	20.28	20.21	22.69	20.84
2/20/2006	23.86	22.96	22.57	21.55	20.42	20.12	20.07	20.05	22.58	20.44
2/27/2006	23.92	23.50	22.56	21.25	20.67	20.26	20.20	20.13	22.58	20.68
3/6/2006	23.79	22.88	22.48	21.21	20.33	20.01	19.97	19.97	22.51	20.33
3/13/2006	23.70	22.80	22.37	21.13	20.19	19.78	19.87	19.90	22.41	20.20
3/20/2006	23.62	22.77	22.29	21.02	20.04	19.77	19.77	19.83	22.30	20.04
3/27/2006	23.54	22.65	22.21	20.97	19.93	19.68	19.68	19.77	22.22	19.94
4/3/2006	23.48	22.59	22.14	20.91	19.87	19.61	19.63	19.75	22.15	19.83
4/10/2006	23.41	22.53	22.08	20.88	19.75	19.57	19.59	19.71	24.62	19.75
4/17/2006	23.33	22.48	22.01	20.97	19.68	19.26	19.53	19.67	22.02	19.67
4/24/2006	23.26	22.40	21.89	20.78	19.61	19.31	19.47	19.64	21.87	19.92
5/1/2006	23.11	22.34	21.86	20.74	19.45	19.30	19.26	19.37	21.84	19.53
5/8/2006	23.13	22.30	21.80	20.71	19.53	19.38	19.41	19.60	21.79	19.51
5/15/2006	23.07	22.25	21.74	20.70	19.53	19.42	19.44	19.58	21.72	19.51
5/22/2006	23.09	22.20	21.76	20.80	19.70	19.51	19.52	19.67	21.74	19.69
5/28/2006	23.02	22.17	21.69	20.72	19.51	19.34	19.36	19.53	21.67	19.50
6/5/2006	22.96	22.12	21.62	20.65	19.45	19.19	19.16	19.25	21.60	19.44
6/13/2006	23.78	22.65	22.43	20.94	20.82	20.37	20.31	20.29	22.46	20.82
6/21/2006	23.63	22.72	22.35	21.21	20.22	19.89	19.87	19.93	22.35	20.20
7/6/2006	24.25	23.41	22.97	21.58	20.87	20.37	20.30	20.29	23.03	20.86
8/29/2006	24.57	23.80	23.29	21.98	20.95	20.33	20.24	20.07	23.37	20.86

Table 5. Head elevation data cont. (m)

	PS-54	USF-1S	USF-2S	USF-3S	USF-4S	USF-6S	USF-7S	USF-8S	USF-9S	Stream
1/23/2006	19.97	23.77	23.95	22.44	21.51	20.25	19.95	19.26	20.11	
1/30/2006	19.95	23.66	23.90	24.34	21.47	20.11	19.88	19.95	19.96	
2/6/2006	20.35	24.05	24.22	22.70	21.37	20.84	20.12	20.29	20.12	19.96
2/20/2006	20.11	23.87	24.12	22.59	21.40	20.42	20.14	20.06	19.98	19.92
2/27/2006	20.26	23.93	23.50	22.60	21.34	20.70	20.06	20.20	20.03	19.93
3/6/2006	20.00	23.80	24.06	22.53	21.33	20.32	19.99	19.96	19.96	19.92
3/13/2006	19.89	23.72	23.98	22.45	21.32	20.19	19.85	19.85	19.94	19.91
3/20/2006	19.77	23.49	23.90			20.04	19.74	19.74	19.91	19.91
3/27/2006	19.68		23.83				19.66	19.67	19.89	19.90
4/3/2006	19.60		23.77		21.31		19.60	19.60	19.86	19.90
4/10/2006	19.56							19.57	19.86	19.90
4/17/2006	19.74								19.84	19.90
4/24/2006	19.45								19.83	19.89
5/1/2006	19.30								21.22	
5/8/2006	19.37								19.86	19.89
5/15/2006	19.39								19.76	
5/22/2006	19.48								19.85	
5/28/2006	19.31								19.73	
6/5/2006	19.16								21.22	
6/13/2006	20.36	23.78	23.84	22.59		20.84	19.93	20.33	20.24	20.09
6/21/2006	19.88	23.64	23.90			20.22	19.95	19.84	19.99	20.03
7/6/2006	20.36	24.27	24.65	23.06		20.89	20.03	20.31	20.25	20.26
8/29/2006	20.31	24.58	24.98	23.39	21.49	20.98	20.28	20.25	20.09	20.15

Table 6. Ground-water conductivity data (uS/cm)

	USF-1D	USF-2D	USF-3D	USF-4D	USF-6D	USF-7D	USF-8D	USF-9D	PS-51	PS-53
1/23/2006	85	107.5	280		283	541	320	157	56	342
1/30/2006	163	166	271	259	241	518	297	160	55.7	340
2/6/2006	108	252	283	244	263	517	303	135	58	265
2/20/2006	277	346	260	282	237	471	281	139	66.5	290
2/27/2006		309	273	246	218	435	297	160	64.6	260
3/6/2006	246	329	296	273	265	431	315	184	72	287
3/13/2006	222	339	284	263	252	428	310	199	68.9	293
3/20/2006	228	345	280	261	253	425	316	188	70	328
3/27/2006	219	362	277	260	239	464	311	156.5	69.8	336
4/3/2006	232	355	276	258	244	506	308	172.6	72.5	355
4/17/2006	278	369	258	239	199.2	480	258	161.1	69.6	362
4/24/2006	243	328	268	264	216	472	267	163.7	71.5	373
5/1/2006	278	345	262	267	234	457	224	148	71.3	357
5/8/2006	262	372	250	256	219	423	226	123.2	68	322
5/15/2006	288	352	245	262	225	430	188.2	143	61.2	347
5/22/2006	175	376	257	263	229	417	183.6	160.7	64	319
5/28/2006	231	365	250		235	413	188.8	168.7	63.6	333
6/5/2006	236	334	237	262	230	401	184	135.4	66.5	338
6/13/2006	205	359	282	269	276	425	220	605	94.4	273
6/21/2006	266	399	283	267	285	386	219	147	89	307
7/6/2006	125	119	189	279	239	296	216	221	67	
8/29/2006	93	248	210	267	204	502	278	168.8	64.6	193

Table 7. Ground-water conductivity data cont. (uS/cm)

	PS-54	USF-1S	USF-2S	USF-3S	USF-4S	USF-6S	USF-7S	USF-8S	USF-9S	Stream
1/23/2006	469	126.3	257					293	217	239
1/30/2006	455	206	197		485	350	576	281	244	177.2
2/6/2006	486	130	379	370	775	301	364	274	206	254
2/20/2006	471	252	340	299	840	285	389	295	227	162.8
2/27/2006	478	244	348	341	890	268		301	193	171.4
3/6/2006	458	269	366	347		292	416	305	193.6	143
3/13/2006	446	255	370	296		262	381	309	192	150
3/20/2006	429	212	383			264	440	301	195.4	139.9
3/27/2006	411		271					314	196.6	138.4
4/3/2006	417		243					317	179.5	153.4
4/17/2006	437								192.2	124.3
4/24/2006	454								271	125.7
5/1/2006	467									
5/8/2006	461								367	346
5/15/2006	464								335	
5/22/2006	450								280	343
5/28/2006	444								402	
6/5/2006	425									
6/13/2006	443	139.6		399		325	1470	473	613	283
6/21/2006	425	148	253			242	1200	349	571	334
7/6/2006	434	109	106	224		232	550	243	272	152
8/29/2006	718	160.4	295	184.8	2130	234	365	274	274	199

Table 8. Conductivity data (uS/cm) from EM 31.

	Mar-05			May-06		
From USF1 to river (m)	L1	L2	L3	L4	L5	L6
0	60	100	130	59	82	101
10	70	80	100	61	80	91
20	70	80	90	66	74	94
30	80	70	90	65	67	91
40	80	80	80	62	65	95
50	80	70	80	58	63	85
60	80	80	90	57	60	89
70	70	80	80	58	59	89
80	80	70	90	61	58	94
90	80	80	90	56	64	102
100	70	60	90	61	66	88
110	70	50	100	64	65	98
120	70	60	120	70	58	102
130	70	50	120	72	54	107
140	80	50	110	74	55	118
150	80	70	120	76	57	119
160	90	70	140	78	58	124
170	80	80	150	73	62	107
180	80	90	160	76	64	124
190	90	100	180	88	72	116
200	100	120	180	90	80	112
210	110	130	170	104	88	118
220	110	150	170	96	102	139
230	110	140	140	105	104	161
240	120	140	120	112	105	169
250	110	160	120	116	113	198
260	130	140	140	123	122	221
270	150	130	180	142	122	208
280	160	120	220	147	119	207
290	160	140	230	153	122	213
300	110	170	210	155	126	231
310	190	180	210	170	134	
320	210	160	210	204	148	169
330	200	160	240	210	157	172
340	200	120	210	184	161	186
350	180	120	190	150	147	185
360			190	121	126	126
370			210			

Appendix D. Results

Table 9. Model conductivity results.

Column #	X coordinate (m)	Concentration uS/cm Layer 1	Layer 2	Layer 3	Layer 4
1	5	-1	-1	455.794	286.021
2	15	-1	-1	513.004	213.928
3	25	-1	-1	456.707	165.689
4	35	-1	-1	380.499	133.673
5	45	-1	-1	310.84	111.658
6	55	-1	-1	253.299	96.6434
7	65	-1	-1	207.38	86.5459
8	75	-1	-1	171.251	79.8999
9	85	-1	-1	143.216	75.4272
10	95	-1	-1	121.273	72.2161
11	105	-1	-1	103.584	69.8647
12	115	-1	75.8216	88.9289	67.8043
13	125	-1	71.8422	83.9395	64.994
14	135	-1	71.6567	82.3351	63.2318
15	145	-1	73.0213	82.013	61.9072
16	155	-1	74.9106	82.1915	60.8012
17	165	-1	76.8214	82.5431	59.7989
18	175	-1	78.5579	82.8956	58.8578
19	185	-1	79.9986	83.2127	57.946
20	195	-1	81.104	83.4779	57.0563
21	205	-1	81.8507	83.6889	56.1926
22	215	-1	82.2452	83.7139	55.2927
23	225	-1	86.5417	83.4736	53.8907
24	235	-1	93.0831	79.6108	50
25	245	-1	100.565	87.6254	-1
26	255	-1	108.373	90.9126	-1
27	265	208.944	117.098	91.8605	-1
28	275	202.275	114.968	91.8455	-1
29	285	198.586	111.658	91.5788	-1
30	295	193.105	107.877	91.2528	-1
31	305	185.648	104.215	90.9506	-1
32	315	176.627	100.958	90.7111	-1
33	325	166.531	98.2202	90.537	-1
34	335	155.747	96.0281	90.4172	-1
35	345	144.67	94.3353	90.3318	-1
36	355	133.512	93.0952	90.2711	-1
37	365	122.467	92.2495	90.2098	-1
38	375	111.668	91.7165	90.1446	-1
39	385	101.11	91.3086	90.0855	-1
40	395	90	90	90	-1

Table 10. Numerical model mass balance results.

Type	row	column	layer	timestep	stressperiod	segment	reach	flux (concentration)	segment	flux (water)	head
Recharge inflow	1	1	1	10	1	0.00E+00			8.45E-01		
Recharge outflow	1	1	1	10	1	0.00E+00			0.00E+00		
ET inflow	1	1	1	10	1	0	0	0.00E+00	0	0.00E+00	
ET outflow	1	1	1	10	1	0	0	0.00E+00	0	9.12E-01	
Qz Top inflow	1	1	1	10	1	0	0	0.00E+00	0	0.00E+00	
Qz Top outflow	1	1	1	10	1	0	0	0.00E+00	0	0.00E+00	
Qz Bottom inflow	1	1	1	10	1	0	0	0.00E+00	0	0.00E+00	
Qz Bottom outflow	1	1	1	10	1	0	0	1.40E+02	0	1.29E+00	
Storage inflow	1	1	1	10	1	0	0	0.00E+00	0	1.42E-06	
Storage outflow	1	1	1	10	1	0	0	0.00E+00	0	0.00E+00	
CH	1	40	1	10	1	0	0	1.22E+02	0	1.36E+00	2.43E+01
Total IN	1	1	1	10	1	0	0	1.22E+02	0	2.21E+00	
Total OUT	1	1	1	10	1	0	0	1.40E+02	0	2.20E+00	
Recharge inflow	1	1	1	10	1	0.00E+00			9.75E-01		
Recharge outflow	1	1	1	10	1	0.00E+00			0.00E+00		
ET inflow	1	1	1	10	1	0	0	0.00E+00	0	0.00E+00	
ET outflow	1	1	1	10	1	0	0	0.00E+00	0	3.41E-01	
Qz Top inflow	1	1	2	10	1	0	0	1.21E+02	0	1.29E+00	
Qz Top outflow	1	1	2	10	1	0	0	0.00E+00	0	0.00E+00	
Qz Bottom inflow	1	1	2	10	1	0	0	0.00E+00	0	0.00E+00	
Qz Bottom outflow	1	1	2	10	1	0	0	1.66E+02	0	1.92E+00	
Storage inflow	1	1	2	10	1	0	0	0.00E+00	0	1.80E-06	
Storage outflow	1	1	2	10	1	0	0	0.00E+00	0	3.88E-06	
CH	1	40	2	10	1	0	0	0.00E+00	0	0.00E+00	2.43E+01
Total IN	1	1	2	10	1	0	0	1.21E+02	0	2.27E+00	
Total OUT	1	1	2	10	1	0	0	1.66E+02	0	2.26E+00	
Recharge inflow	1	1	1	10	1	0.00E+00			4.95E-06		
Recharge outflow	1	1	1	10	1	0.00E+00			0.00E+00		

Table 11. Numerical model mass balance results cont.

Type	row	column	layer	timestep	stressperiod	segment	reach	flux (concentration)	segment	flux (water)	head
ET inflow	1	1	1	10	1	0	0	0.00E+00	0	0.00E+00	
ET outflow	1	1	1	10	1	0	0	0.00E+00	0	1.63E+00	
Qz Top inflow	1	1	3	10	1	0	0	1.65E+02	0	1.92E+00	
Qz Top outflow	1	1	3	10	1	0	0	0.00E+00	0	0.00E+00	
Qz Bottom inflow	1	1	3	10	1	0	0	3.04E+02	0	9.55E-01	
Qz Bottom outflow	1	1	3	10	1	0	0	7.81E+01	0	9.52E-01	
Storage inflow	1	1	3	10	1	0	0	0.00E+00	0	1.82E-06	
Storage outflow	1	1	3	10	1	0	0	0.00E+00	0	5.58E-06	
River	1	1	3	10	1	0	1	-1.35E+02	0	-2.97E-01	2.01E+01
CH	1	40	3	10	1	0	0	0.00E+00	0	0.00E+00	2.43E+01
Total IN	1	1	3	10	1	0	0	4.70E+02	0	2.88E+00	
Total OUT	1	1	3	10	1	0	0	2.13E+02	0	2.88E+00	
Recharge inflow	1	1	1	10	1	0.00E+00			0.00E+00		
Recharge outflow	1	1	1	10	1	0.00E+00			0.00E+00		
ET inflow	1	1	1	10	1	0	0	0.00E+00	0	0.00E+00	
ET outflow	1	1	1	10	1	0	0	0.00E+00	0	0.00E+00	
Qz Top inflow	1	1	4	10	1	0	0	5.30E+01	0	9.52E-01	
Qz Top outflow	1	1	4	10	1	0	0	1.50E+02	0	9.55E-01	
Qz Bottom inflow	1	1	4	10	1	0	0	0.00E+00	0	0.00E+00	
Qz Bottom outflow	1	1	4	10	1	0	0	0.00E+00	0	0.00E+00	
Storage inflow	1	1	4	10	1	0	0	0.00E+00	0	0.00E+00	
Storage outflow	1	1	4	10	1	0	0	0.00E+00	0	5.60E-06	
CH	1	24	4	10	1	0	0	0.00E+00	0	0.00E+00	2.27E+01
Total IN	1	1	4	10	1	0	0	5.30E+01	0	9.52E-01	
Total OUT	1	1	4	10	1	0	0	1.50E+02	0	9.55E-01	
Grand Total IN	0	0	0	0	0	122.4648			3.180729		
Grand Total OUT	0	0	0	0	0	135.2138			3.179766		
Grand Total ERROR	0	0	0	0	0	-9.89529			0.030298		